An Efficient PMU-based Fault Location Technique for Multi-Terminal Transmission Lines

Quanyuan Jiang, *Member, IEEE*, Bo Wang, Xingpeng Li

***Abstract*—This paper presents a new fault location technique for multi-terminal transmission lines using phasor measurement unit (PMU). A two-stage fault location model is proposed, along with defining nodal current unbalance, a fault location index. The first stage is the fault line selector stage, which uses the non-zero elements of nodal current unbalance to determine the fault line. The second stage is used to identify the exact fault distance. The computational burden of the proposed technique is very low because it provides an analytical solution and avoids iterative computations. The performance of this technique is thoroughly evaluated under various fault conditions. Very promising simulation results verify the accuracy and robustness of the proposed technique for multi-terminal transmission lines.**

***Index Terms*—Fault location, multi-terminal transmission line, nodal current unbalance, phasor measurement unit.**

I. Introduction

Accurate fault location on a transmission line can expedite repair of the faulted components, speed-up restoration, reduce outage time, and thus improve power system reliability [1]. Till now, the most common methods are one-terminal method and two-terminal method. One-terminal methods only use one-terminal voltage and current phasors, so the accuracies of fault location are normally adversely affected by the fault resistance and remote-terminal system impedance [2-5]. To improve the accuracy of fault location, two-terminal algorithms are developed [6-9].

With the development of modern power system, the transmission network is becoming more and more complicated. Three terminal and multi-terminal transmission lines inevitably appear and the existing one-terminal or two-terminal fault location algorithms are unable to determine which branch the fault occurs on. Several fault location methods for three terminal transmission lines have been proposed [10-13]. However, due to the complexity of the problem, only a few algorithms [14-18] for fault location in multi-terminal transmission lines have been proposed. Abe et al. [14] used a reactive power-based method to locate the exact fault position after the multi-terminal line was reduced into a two-terminal line containing the fault section. Funabashi et al. [15] used two different methods to locate the fault. However, results for three-phase and two-phase to ground faults weren't reported. Sanderson et al. [16] can successfully identify the faulted section, but the exact fault location on the faulted section was not studied. Chih-Wen Liu et al [17] extended a two-terminal fault location technique to N-terminal transmission lines. It is suitable for any type of multi-terminal line. But, (N-1) two-terminal indices should be calculated, which increases the computational burden. Brahma [18] reported successful results by only using voltage measurements to locate fault, but the exact power source impedances must be available. The source impedances at line terminals are also required in [19-20].

For multi-terminal transmission lines, the main difficulty of fault location is to identify the faulted section. Once the faulted section is identified, the fault point can be located easily. These existing methods [14-18] may bring heavy computational burden or require source impedances to identify the faulted section. Therefore, a multi-terminal fault location technique can be promising when it is with low computational burden and avoids the use of source impedances. To achieve this objective, nodal current unbalance is defined firstly, and then used as a fault location index in this paper. Based on this index, a novel fault section selector is proposed to locate the fault on a multi-terminal transmission line. Simulation studies verify that the proposed technique is accurate and efficient under different fault conditions.

II. The Proposed Fault Location Index

A. Generating the fault location index

Considering n–terminal transmission line depicted in Fig. 1, all nodes are classified into two types: terminal node p ($p = 1, 3, 5, ..., n-3, n-1, n$), and tap node q ($q = 2, 4, 6, ..., n-4, n-2$). We assume that every terminal node is equipped with a PMU; this assumption is common in the literature [14-18]. Therefore, the synchronized voltage and current phasors at all terminals are available.

Because the positive sequence is the only network sequence for all types of faults, the positive sequence measurements are utilized in this paper. All the quantities, if not specifically labeled, refer to positive sequence quantities. It is assumed that the transmission lines to be considered are transposed.

This work was supported by the National Key Basic Research and Development Program (973 Program) of China (Grant No. 2012CB215106), and the National High Technology Research and Development Program ("863"Program) of China (Grant No. 2011AA05A113).

Quanyuan Jiang is with College of Electrical Engineering, Zhejiang University, Hangzhou 310027, China (email: jqy@zju.edu.cn)

Bo Wang is with Ningbo Electric Company of State Grid, Ningbo 315000, China (email: zjuwangbo@gmail.com)

Xingpeng Li is with College of Electrical Engineering, Zhejiang University, Hangzhou 310027, China (email: xplipower@gmail.com)

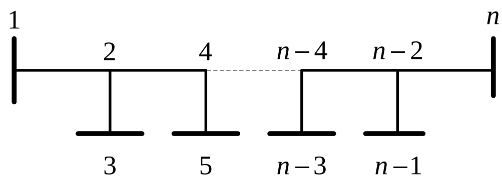

Fig.1. *n*-terminal transmission line system

In Fig.1, the pre-fault state of the *n*-terminal system can be represented by the node admittance equation:

$$\mathbf{Y}_{n\times n}\mathbf{U}^0{}_{n\times 1}=\mathbf{I}^0{}_{n\times 1} \tag{1}$$

Where, $\mathbf{U}^0{}_{n\times 1}$ is pre-fault node voltage vector; $\mathbf{I}^0{}_{n\times 1}$ is the pre-fault node current injection vector; $\mathbf{Y}_{n\times n}$ is pre-fault bus-admittance matrix. Fig.2 shows the π equivalent model used in this paper of line section $i-j$.

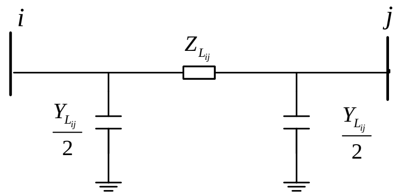

Fig.2. π equivalent model of line section $i-j$

In this model, $Z_{L_{ij}}$ is equivalent impedance of the line $i-j$. The effect of shunt capacitances is taken into account by admittance $Y_{L_{ij}}$. In order to introduce the fault location index, a fault on the line section $i-j$ is shown in Fig.3.

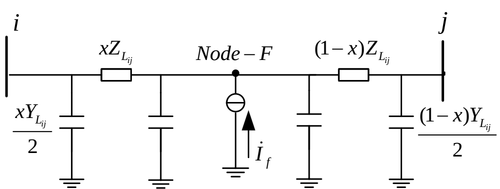

Fig.3. a fault occurs on the line section $i-j$

The fault node-F can be treated as a fictitious node, thus the line is equivalent as two π models. The unknown variable *x* is defined as the percent that the fault distance from node *i* to fault node F of the line length. Obviously *x* varies from 0 to 1, which is to be solved in the paper.

Let $F=n+1$, the post-fault system would yield a new bus-admittance matrix with the dimension of $(n+1)$:

$$\mathbf{Y}_{new}=\begin{bmatrix} Y_{11} & \dots & Y_{1i} & \dots & Y_{1j} & \dots & Y_{1n} & 0 \\ \dots & \dots & \dots & \dots & \dots & \dots & \dots & 0 \\ Y_{i1} & \dots & Y_{ii}^{'} & \dots & Y_{ij}^{'} & \dots & Y_{in} & Y_{i(n+1)}^{'} \\ \dots & \dots & \dots & \dots & \dots & \dots & \dots & 0 \\ Y_{j1} & \dots & Y_{ji}^{'} & \dots & Y_{jj}^{'} & \dots & Y_{jn} & Y_{j(n+1)}^{'} \\ \dots & \dots & \dots & \dots & \dots & \dots & \dots & 0 \\ Y_{n1} & \dots & Y_{ni} & \dots & Y_{nj} & \dots & Y_{nn} & 0 \\ 0 & 0 & Y_{(n+1)i}^{'} & 0 & Y_{(n+1)j}^{'} & 0 & 0 & Y_{(n+1)(n+1)}^{'} \end{bmatrix} \tag{2}$$

The elements in $\mathbf{Y}_{new}$ related to node *i* and node *j* are different from those in the original matrix $\mathbf{Y}_{n\times n}$, Equations (3)–(8) describe this difference:

$$Y_{ii}^{'}=Y_{ii}-\frac{Y_{L_{ij}}}{2}-\frac{1}{Z_{L_{ij}}}+\frac{xY_{L_{ij}}}{2}+\frac{1}{xZ_{L_{ij}}} \tag{3}$$

$$Y_{ij}^{'}=Y_{ji}^{'}=0 \tag{4}$$

$$Y_{i(n+1)}^{'}=Y_{(n+1)i}^{'}=-\frac{1}{xZ_{L_{ij}}} \tag{5}$$

$$Y_{jj}^{'}=Y_{jj}-\frac{Y_{L_{ij}}}{2}-\frac{1}{Z_{L_{ij}}}+\frac{(1-x)Y_{L_{ij}}}{2}+\frac{1}{(1-x)Z_{L_{ij}}} \tag{6}$$

$$Y_{j(n+1)}^{'}=Y_{(n+1)j}^{'}=-\frac{1}{(1-x)Z_{L_{ij}}} \tag{7}$$

$$Y_{(n+1)(n+1)}^{'}=\frac{Y_{L_{ij}}}{2}+\frac{1}{xZ_{L_{ij}}}+\frac{1}{(1-x)Z_{L_{ij}}} \tag{8}$$

Except the above elements, the other elements in $\mathbf{Y}_{n\times n}$ and $\mathbf{Y}_{new}$ are the same.

Hence, when a fault occurs on the line $i-j$, the following equation can be formed:

$$\boldsymbol{Y}_{new}\begin{bmatrix}\boldsymbol{U}_{n\times 1}\\ U_f\end{bmatrix}=\begin{bmatrix}\boldsymbol{I}_{n\times 1}\\ I_f\end{bmatrix} \tag{9}$$

Where, U_f, I_f are the node voltage and current injection at fault point F respectively; $\boldsymbol{U}_{n\times 1}$ is the post-fault node voltage vector; $\boldsymbol{I}_{n\times 1}$ is the post-fault node current vector.

For the i^{th} and j^{th} rows in (9), we have:

$$Y_{i1}U_1+\dots+Y_{ii}^{'}U_i+\dots+Y_{ij}^{'}U_j+\dots+Y_{in}U_n+Y_{i(n+1)}^{'}U_f=I_i \tag{10}$$

$$Y_{j1}U_1+\dots+Y_{ji}^{'}U_i+\dots+Y_{jj}^{'}U_j+\dots+Y_{jn}U_n+Y_{j(n+1)}^{'}U_f=I_j \tag{11}$$

Equation (10) and (11) can be modified as follows:

$$\begin{aligned} &Y_{i1}U_1+\dots+Y_{ii}U_i+\dots+Y_{ij}U_j+Y_{in}U_n= \\ &\qquad I_i+(Y_{ii}-Y_{ii}^{'})U_i+(Y_{ij}-Y_{ij}^{'})U_j-Y_{i(n+1)}^{'}U_f \end{aligned} \tag{12}$$

$$\begin{aligned} &Y_{j1}U_1+\dots+Y_{ji}U_i+\dots+Y_{jj}U_j+Y_{jn}U_n= \\ &\qquad I_j+(Y_{ji}-Y_{ji}^{'})U_i+(Y_{jj}-Y_{jj}^{'})U_j-Y_{j(n+1)}^{'}U_f \end{aligned} \tag{13}$$

For convenience, equation (12) and (13) are simplified as:

$$Y_{i1}U_1+\dots+Y_{ii}U_i+\dots+Y_{ij}U_j+Y_{in}U_n=I_i+\Delta I_i \tag{14}$$

$$Y_{j1}U_1+\dots+Y_{ji}U_i+\dots+Y_{jj}U_j+Y_{jn}U_n=I_j+\Delta I_j \tag{15}$$

Where,

$$\Delta I_i=(Y_{ii}-Y_{ii}^{'})U_i+(Y_{ij}-Y_{ij}^{'})U_j-Y_{i(n+1)}^{'}U_f \tag{16}$$

$$\Delta I_j=(Y_{ji}-Y_{ji}^{'})U_i+(Y_{jj}-Y_{jj}^{'})U_j-Y_{j(n+1)}^{'}U_f \tag{17}$$

Except the i^{th}, j^{th} and $(n+1)^{th}$ rows, the other rows in (9) can be written as follows:

$$Y_{k1}U_1+\dots+Y_{ki}U_i+\dots+Y_{kj}U_j+Y_{kn}U_n=I_k \tag{18}$$

Where, $k=1,2,\dots,i-1,i+1,\dots,j-1,j+1,\dots,n-1,n$.

From (14), (15) and (18), the following equation can be established:

$$\begin{bmatrix} Y_{11} & \dots & Y_{1i} & \dots & Y_{1j} & \dots & Y_{1n} \\ \dots & \dots & \dots & \dots & \dots & \dots & \dots \\ Y_{i1} & \dots & Y_{ii} & \dots & Y_{ij} & \dots & Y_{in} \\ \dots & \dots & \dots & \dots & \dots & \dots & \dots \\ Y_{j1} & \dots & Y_{ji} & \dots & Y_{jj} & \dots & Y_{jn} \\ \dots & \dots & \dots & \dots & \dots & \dots & \dots \\ Y_{n1} & \dots & Y_{ni} & \dots & Y_{nj} & \dots & Y_{nn} \end{bmatrix} \begin{bmatrix} U_1 \\ \dots \\ U_i \\ \dots \\ U_j \\ \dots \\ U_n \end{bmatrix} = \begin{bmatrix} I_1 \\ \dots \\ I_i + \Delta I_i \\ \dots \\ I_j + \Delta I_j \\ \dots \\ I_n \end{bmatrix} \tag{19}$$

Equation (19) can be rewritten as follows:

$$\mathbf{Y}_{n\times n}\mathbf{U}_{n\times 1} = \mathbf{I}_{n\times 1} + \Delta\mathbf{I}_{n\times 1} \tag{20}$$

Where

$$\Delta\mathbf{I}_{n\times 1} = \begin{bmatrix} 0, \dots, & 0, & \Delta I_i, & 0, & \Delta I_j, & 0, \dots, & 0 \end{bmatrix}^T \tag{21}$$

From (21), we can observe the following characteristic: when a fault occurs on the line section $i-j$, $\Delta\mathbf{I}_{n\times 1}$ has only two non-zero elements ΔI_i and ΔI_j. By checking the non-zero elements of $\Delta\mathbf{I}_{n\times 1}$, we can identify the faulted line section.

Hence, $\Delta\mathbf{I}_{n\times 1}$ is defined as nodal current unbalance in (21), which will provide a simple and efficient index to locate the faulted section in multi-terminal lines.

From (20), in order to obtain $\Delta\boldsymbol{I}_{n\times 1}$, $\boldsymbol{U}_{n\times 1}$ and $\boldsymbol{I}_{n\times 1}$ must be known. When a fault occurs on the system in Fig.1, the voltage U_p and injected current I_p at every terminal node p ($p = 1, 3, 5, \dots, n-3, n-1, n$) are measured by PMU, and the current injection I_q at tap node q ($q = 2, 4, 6, \dots, n-4, n-2$) is zero, so $\boldsymbol{I}_{n\times 1}$ and U_p ($p = 1, 3, 5, \dots, n-3, n-1, n$) are known, only the voltage U_q at the tap node q ($q = 2, 4, 6, \dots, n-4, n-2$) is unknown.

In order to obtain U_q, we firstly assume that the fault only occurs on the main line section (line 1-2, 2-4, 4-6, etc). From the geometry of the multi-terminal lines in Fig.1, the following equation can be derived for terminal node p ($p = 3, 5, \dots, n-3, n-1$):

$$Y_{pp}U_p + Y_{p(p-1)}U_{p-1} = I_p \tag{22}$$

Since U_{p-1} is the sole unknown variable in (22), it can be easily obtained as follows:

$$U_{p-1} = (I_p - Y_{pp}U_p)/Y_{p(p-1)} \tag{23}$$

Because $\boldsymbol{I}_{n\times 1}$ and U_p ($p = 1, 3, 5, \dots, n-3, n-1, n$) are known by PMU measurements, so we can compute the voltage U_{p-1} of tap node by (23). Once $\boldsymbol{U}_{n\times 1}$ and $\boldsymbol{I}_{n\times 1}$ are obtained, then $\Delta\mathbf{I}_{n\times 1}$ can be calculated by using (24).

$$\Delta\boldsymbol{I}_{n\times 1} = \boldsymbol{Y}_{n\times n}\boldsymbol{U}_{n\times 1} - \boldsymbol{I}_{n\times 1} \tag{24}$$

However, the fault may also occur on tapped line section (line 2-3, 4-5, 6-7, etc). in this case, the assumption is not satisfied. So we will discuss its application in the following two cases: a fault occurs on the main line section, and a fault occurs on the tapped line section. For each case, $\Delta\mathbf{I}_{n\times 1}$ have different characteristics.

B. Fault on the main line section

As shown in Fig.4, the fault occurs on the main line section (line 1-2, 2-4, 4-6, etc). In this case, the assumption holds. So, the unknown voltages at all the tap nodes can be calculated by (23) correctly.

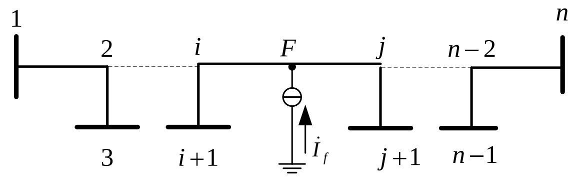

Fig.4. a fault occurs on the main line section *i* - *j*.

If a fault occurs on the main line section $i-j$, obviously the computed fault location index $\Delta\mathbf{I}_{n\times 1}$ will only have two nonzero elements as shown in Eq. (21).

More specifically, in Fig.1, main line sections consist of line $1-2$ and $l-(l+2)$ ($l \in 2, 4 \dots n-2$), so $\Delta\mathbf{I}_{n\times 1}$ can be outlined as follows:

$$\Delta\mathbf{I}_{n\times 1} = \begin{cases} \left[\Delta I_1, \Delta I_2, 0, \ \dots, 0\right]^T & \textit{fault on line 1-2} \\ \left[0, \dots, 0, \Delta I_l, 0, \Delta I_{l+2}, 0, \dots, 0\right]^T & \textit{fault on line } l\textit{-}(l+2) \end{cases} \tag{25}$$

C. Fault on the tapped line section

If a fault occurs on the tapped line section (line 2-3, 4-5, 6-7, etc) such as the tapped line $i-j$ as shown in Fig.5, the assumption does not hold. The voltage $U_i^{'}$ at tap node i is calculated by (23) and the fault current I_f is not considered. So the calculated $U_i^{'}$ is not the true voltage U_i of tap node i, i.e. $U_i^{'} \neq U_i$. In this case, $\Delta\mathbf{I}_{n\times 1}$ has different characteristic.

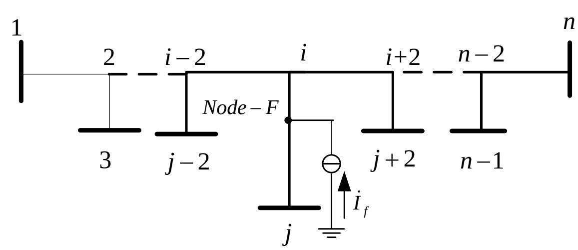

Fig.5. a fault occurs on the tapped line section *i* - *j*.

In Fig.5, the calculated voltage $U_i^{'}$ at tap node i is calculated by (23), i.e.:

$$U_i^{'} = (I_j - Y_{jj}U_j)/Y_{ji} \tag{26}$$

Due to the effect of fault current I_f, the calculated voltage $U_i^{'}$ does not equal to the true voltage U_i at tap node i. In this case, we have:

$$\mathbf{U}_{n\times 1} = \begin{bmatrix} U_1 & .. & U_i^{'} & .. & U_j & .. & U_n \end{bmatrix}^T \tag{27}$$

Therefore, $\Delta\mathbf{I}_{n\times 1}$ can also be obtained as follows:

$$\Delta\mathbf{I}_{n\times 1} = \mathbf{Y}_{n\times n}\mathbf{U}_{n\times 1} - \mathbf{I}_{n\times 1}$$

Next, we will analyze all non-zero elements of $\Delta\mathbf{I}_{n\times 1}$ in this case.

- For node i, we have:

$$\Delta I_i = Y_{i1}U_1 + \dots + Y_{ii}U_i^{'} + \dots + Y_{ij}U_j + \dots + Y_{in}U_n - I_i \tag{28}$$

Substitute (10) into (28), we have:

$$\Delta I_i = (Y_{ii}U_i^{'} - Y_{ii}^{'}U_i) + (Y_{ij} - Y_{ij}^{'})U_j - Y_{i(n+1)}^{'}U_f \quad (29)$$

- For node j , we have:

$$\Delta I_j = Y_{j1}U_1 + ... + Y_{ji}U_i^{'} + ... + Y_{jj}U_j + Y_{jn}U_n - I_j \quad (30)$$

Because the j^{th} row in $\mathbf{Y}_{n\times n}$ has only two non-zero elements: Y_{ji} and Y_{jj} , so (30) can be simplified as follows:

$$\Delta I_j = Y_{ji}U_i^{'} + Y_{jj}U_j - I_j \quad (31)$$

Substitute (26) into (31), we have:

$$\Delta I_j = Y_{ji}\,(I_j - Y_{jj}U_j)/Y_{ji} + Y_{jj}U_j - I_j = 0 \quad (32)$$

- For any other node k ($k \neq i$ and $k \neq j$), we have:

$$\Delta I_k = Y_{k1}U_1 + ... + Y_{ki}U_i^{'} + ... + Y_{kj}U_j + ... + Y_{kn}U_n - I_k \quad (33)$$

Substitute (18) into (33), we have:

$$\Delta I_k = Y_{ki}(U_i^{'} - U_i) \quad (34)$$

In Fig.5, only node $(i-2)$ and node $(i+2)$ are directly connected with node i , so $Y_{(i-2)i} \neq 0$, $Y_{(i+2)i} \neq 0$, and $Y_{ki}=0$ for any other node k ($k \neq i-2$ and $k \neq i+2$).

Therefore, we can conclude based on (29), (32) and (34):

$$\begin{cases} \Delta I_k = 0 \quad (k \neq i-2,\, i,\, i+2) \\ \Delta I_{i-2} = Y_{(i-2)i}(U_i^{'} - U_i) \\ \Delta I_i = (Y_{ii}U_i^{'} - Y_{ii}^{'}U_i) + (Y_{ij} - Y_{ij}^{'})U_j - Y_{i(n+1)}^{'}U_f \\ \Delta I_{i+2} = Y_{(i+2)i}(U_i^{'} - U_i) \end{cases} \quad (35)$$

From (35), when the fault occurs on the tapped line $i-j$ shown in Fig.5, $\Delta\mathbf{I}_{n\times 1}$ has three non-zero elements ΔI_{i-2} , ΔI_i , and ΔI_{i+2} :

$$\Delta\mathbf{I}_{n\times 1} = [0,\, ...,\, \Delta I_{i-2},\, 0,\, \Delta I_i,\, 0,\, \Delta I_{i+2},\, ...,\, 0]^T \quad (36)$$

Especially, when a fault occurs on the tapped line 2-3, the two connected nodes would be 1 and 4. Then $\Delta\mathbf{I}_{n\times 1}$ should be written as follows:

$$\Delta\mathbf{I}_{n\times 1} = [\Delta I_1, \Delta I_2, \Delta I_4, 0, ..., 0]^T \quad (37)$$

In summary, that is:

$$\Delta\mathbf{I}_{n\times 1} = \begin{cases} [\Delta I_1, \Delta I_2, \Delta I_4, 0, ..., 0]^T & \textit{fault on tapped line } 2\text{-}3 \\ [0, ..., 0, \Delta I_{i-2}, 0, \Delta I_i, 0, \Delta I_{i+2}, 0 ..., 0]^T & \textit{fault on other tapped line } i-j \end{cases}$$

(38)

III. Identifying Fault Section

Based on the theoretical analysis shown in (25) and (38), we propose a fault section selector for multi-terminal lines, which is illustrated by Fig. 6.

There are three cases for the fault section selector. For every case, $\Delta\mathbf{I}_{n\times 1}$ has different characteristic which can be used to identify the faulted line section:

Case 1: $\Delta\mathbf{I}_{n\times 1}$ has two nonzero elements

For case 1, we can identify that a fault occurs on the main line section, referred to Eq.(25).

More specifically, if the two nonzero elements correspond to node i and j , the fault line section $i-j$ is identified undoubtedly. Actually, it should be line section $1-2$ or $l-(l+2)$ ($l \in 2,4...n-2$) as shown in Fig.1.

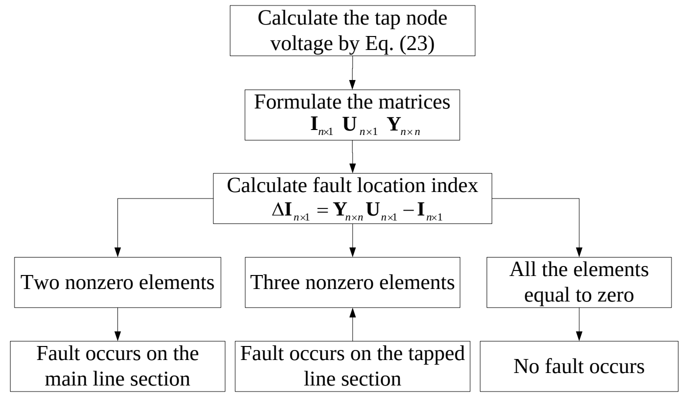

Fig.6. the proposed fault line selector

Case 2: $\Delta\mathbf{I}_{n\times 1}$ has three nonzero elements

For case 2, we can identify that a fault occurs on the tapped line section, referred to Eq.(38).

If the three nonzero elements correspond to nodes n_1 , i and n_2 ($n_1 < i < n_2$), the fault line section $i-j$ is identified. Actually, it should be line section $l-(l+1)$ ($l \in 2,4...n-2$) as shown in Fig.1.

Case 3: every element of $\Delta\mathbf{I}_{n\times 1}$ is zero.

For case 3, we can identify that no fault occurs.

IV. Exact Fault Location

Once the faulted section $i-j$ is identified, the next step is to locate the exact fault point on the faulted section.

Case 1: A fault occurs on the main line section $i-j$.

In this case, the calculated ΔI_i and ΔI_j are non-zero elements, which is given in (16) and (17). Based on (16) and (17), we can eliminate the unknown variable U_f :

$$\begin{aligned} &[\Delta I_i - (Y_{ii} - Y_{ii}^{'})U_i - (Y_{ij} - Y_{ij}^{'})U_j]\,Y_{j(n+1)}^{'} = \\ &\qquad [\Delta I_j - (Y_{ji} - Y_{ji}^{'})U_i - (Y_{jj} - Y_{jj}^{'})U_j]\,Y_{i(n+1)}^{'} \end{aligned} \quad (39)$$

From (3)-(8), we know that $Y_{ii}^{'}$, $Y_{jj}^{'}$, $Y_{i(n+1)}^{'}$ and $Y_{j(n+1)}^{'}$ are functions of fault location variable x . Substitute (3)-(8) into (39), we have the following quadratic equation with one unknown variable x :

$$ax^2 + bx + c = 0 \quad (40)$$

In equation (40), the only variable to be solved is the fault distance x, and $0 \le x \le 1$. The coefficient a, b and c can be calculated as follow:

$$\begin{aligned} a &= k(U_i - U_j) \\ b &= -k(U_i - U_j) + Z_{L_{ij}}(\Delta I_i + \Delta I_j) \\ c &= -\Delta I_j Z_{L_{ij}} \\ k &= \frac{Y_{L_{ij}} Z_{L_{ij}}}{2} \end{aligned} \quad (41)$$

Where, $Y_{L_{ij}}$ and $Z_{L_{ij}}$ are the parameters of π equivalent model of line $i-j$. U_i , U_j are the post-fault voltages at node *i* and *j*, which can be calculated by equation (23).

By solving (40), we can obtain the exact fault point x :

$$x = (-b \pm \sqrt{b^2 - 4ac})/2a \tag{42}$$

Although the solution x can equal to two values in (42), only the solution satisfying $0 \le x \le 1$ is accepted as the fault point.

Case 2: A fault occurs on the tapped line section $i - j$.

In this case, the true voltage U_i of tap node i can be recalculated correctly by using the connected tap node $(i-2)$ or $(i+2)$. For example, we can use tap node $(i-2)$ to obtain U_i:

$$Y_{(i-2)(i-4)}U_{(i-4)} + Y_{(i-2)(i-1)}U_{(i-1)} + Y_{(i-2)(i-2)}U_{(i-2)} + Y_{(i-2)i}U_i = 0 \tag{43}$$

From (43), U_i can be recalculated as follows:

$$U_i = -\left[Y_{(i-2)(i-4)}U_{(i-4)} + Y_{(i-2)(i-1)}U_{(i-1)} + Y_{(i-2)(i-2)}U_{(i-2)}\right] / Y_{(i-2)i} \tag{44}$$

Once U_i is recalculated correctly by (44), $\Delta\mathbf{I}_{n\times1}$ is also recalculated by (24). Then, $\Delta\mathbf{I}_{n\times1}$ will become to have two non-zero elements ΔI_i and ΔI_j, which is a similar problem as *case 1*. Then, the fault point x can also be obtained by (42).

V. Case Studies

A. Simulation system 1

In order to evaluate the proposed fault location algorithm, Power Systems Computer Aided Design (PSCAD) [21] software has been utilized to generate transient waveforms for faults of different types, locations and fault resistances on a 500 kV, 50Hz six-terminal transmission line system, which is shown in Fig. 7. The related parameters of this system are given in Appendix I. The fault location error is defined as follows:

$$Error(\%) = \frac{|\text{Estimated location} - \text{Actual location}|}{\text{The length of faulted section}} \times 100\% \tag{45}$$

To demonstrate the correctness of the developed fault line selector, some typical cases are discussed firstly. Fig.8 shows the calculated index $\Delta\mathbf{I}_{n\times1}$ for a A-phase to ground fault (AG-fault) on the main line 4-6. This fault occurs on the point which is 70% away from node 4 with fault resistance 50 Ω. It can be observed from Fig.8 that ΔI_4 at node 4 and ΔI_6 at node 6 are much larger than zero, while the other current unbalances almost equal to zero. Based on the principle of fault location shown in Fig.6, it can be identified that the fault occurs on the main line section 4-6. Furthermore, the exact fault location x can be obtained by (42): x_1=0.69999, x_2=234.89433. Because $0 \le x \le 1$, so x_1=0.69999=69.999% is the exact fault point. Therefore, the fault location error is 0.001%, which is negligible.

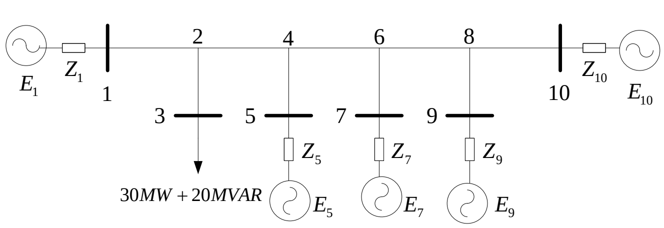

Fig.7. simulated six-terminal transmission lines

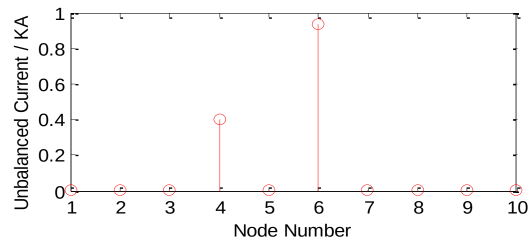

Fig.8. $\Delta\mathbf{I}_{n\times1}$ in *Case 1*- a fault occurs at main line section 4-6

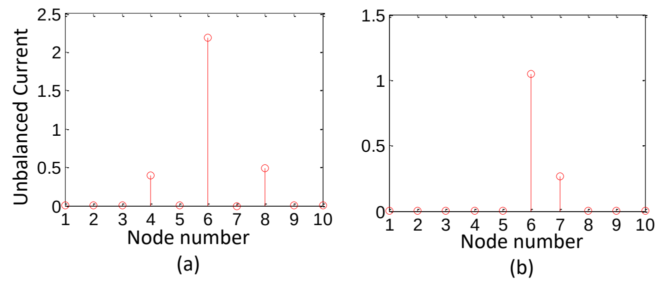

Fig.9. $\Delta\mathbf{I}_{n\times1}$ in *Case 2*- a fault occurs at tapped line section 6-7

Table I All Simulated Faults

Fault section	Fault information			Fault Number
	Fault type	Fault location	Resistance (Ω)	
Line 1-2	AG	5% from 1	100	1
	ABG	50% from 1	50	2
	ABC	95% from 1	100	3
Line 2-3	ACG	5% from 2	1	4
	BG	50% from 2	10	5
	ABC	95% from 2	200	6
Line 2-4	CG	5% from 2	50	7
	BC	50% from 2	200	8
	ABG	95% from 2	500	9
Line 4-5	BCG	5% from 4	200	10
	ABC	50% from 4	10	11
	AB	95% from 4	1	12
Line 4-6	BCG	5% from 4	50	13
	ABG	50% from 4	100	14
	AG	95% from 4	200	15
Line 6-7	BC	5% from 6	500	16
	AC	50% from 6	1	17
	BCG	95% from 6	100	18
Line 6-8	AC	5% from 6	20	19
	BC	50% from 6	50	20
	ACG	95% from 6	5	21
Line 8-9	BC	5% from 8	50	22
	CG	50% from 8	100	23
	BG	95% from 8	200	24
Line 8-10	CG	5% from 8	1000	25
	ACG	50% from 8	50	26
	ABC	95% from 8	20	27

* ABG denotes A and B-phase to ground.
* AG denotes A-phase to ground.
* AB denotes two-phase short circuit.
* ABC denotes three-phase short circuit to ground

Fig.9 (a) shows the calculated index $\Delta\mathbf{I}_{n\times1}$ for a A-phase to ground fault (AG-fault) on the tapped line section 6-7. The fault occurs on the point which is 20% away from node 6 with fault resistance 50 Ω. It can be observed from Fig.9 (a) that the current unbalances ΔI_4 at node 4, ΔI_6 at node 6, and ΔI_8 at node 8 are much larger than zero. Based on the principle of fault location shown in Fig.6, it can be identified that the fault occurs on the tapped line section 6-7.

Once the tapped line section 6-7 is identified as faulted section, the correct voltage U_6 at node 6 can be calculated by (44). Then $\Delta \mathbf{I}_{n\times 1}$ can be recalculated by (24), shown in Fig.9 (b). From Fig.9 (b), ΔI_6 and ΔI_7 are much larger than zero. Using ΔI_6 , ΔI_7 , U_6 and U_7 , we can obtain the exact fault point x by solving (42): x_1=19.997% , x_2=241.64668 . Obviously, x_1=19.997% is the fault point. Therefore, the fault location error is 0.003%, which is pretty small.

To validate the robustness of the proposed fault location technique, more faults are simulated. Table I gives all tested faults. These faults in Table I cover all possible line sections and different types of faults with various fault resistances.

TABLE II
SIMULATION RESULTS UNDER DIFFERENT FAULT CONDITIONS

Fault Number	Fault location index ΔI_i ($i = 1, 2, ..., 10$) 1 2 3 4 5 6 7 8 9 10	Fault section selector	Fault point locator	Error (%)
1	●●○○○○○○○○	Line 1-2	5.00	0
2	●●○○○○○○○○	Line 1-2	50.00	0
3	●●○○○○○○○○	Line 1-2	95.00	0
4	●●○●○○○○○○	Line 2-3	5.00	0
5	●●○●○○○○○○	Line 2-3	49.99	0.01
6	●●○●○○○○○○	Line 2-3	95.00	0
7	○●○●○○○○○○	Line 2-4	5.00	0
8	○●○●○○○○○○	Line 2-4	50.00	0
9	○●○●○○○○○○	Line 2-4	94.99	0.01
10	○●○●○●○○○○	Line 4-5	4.99	0.01
11	○●○●○●○○○○	Line 4-5	50.00	0
12	○●○●○●○○○○	Line 4-5	95.00	0
13	○○○●○●○○○○	Line 4-6	5.00	0
14	○○○●○●○○○○	Line 4-6	50.00	0
15	○○○●○●○○○○	Line 4-6	95.00	0
16	○○○●○●○●○○	Line 6-7	5.00	0
17	○○○●○●○●○○	Line 6-7	50.00	0
18	○○○●○●○●○○	Line 6-7	95.00	0
19	○○○○○●○●○○	Line 6-8	5.00	0
20	○○○○○●○●○○	Line 6-8	50.00	0
21	○○○○○●○●○○	Line 6-8	95.00	0
22	○○○○○●○●○●	Line 8-9	5.00	0
23	○○○○○●○●○●	Line 8-9	49.99	0.01
24	○○○○○●○●○●	Line 8-9	94.98	0.02
25	○○○○○○○●○●	Line 8-10	4.99	0.01
26	○○○○○○○●○●	Line 8-10	50.00	0
27	○○○○○○○●○●	Line 8-10	95.00	0

*○ represents zero element.

*● represents non-zero element.

* All 0 error means that the error is less than 0.01%.

The fault location results using the proposed technique are given in Table II.

As seen from Table II, the proposed fault location algorithm provides excellent performance for all considered faults and it isn't affected by different fault types, fault positions, and fault resistances. The maximum fault location error under various fault conditions is well below 0.1%.

The fault location results under different source impedances of node 1 are given in Table III. In Table III, a phase-A to ground fault occurs on the main line section 2-4, and the fault point is 50% away from node 2. As seen from Table III, the proposed fault location technique is independent of source impedances.

TABLE III
SIMULATION RESULTS UNDER DIFFERENT FAULT CONDITIONS

Fault location index ΔI_i ($i = 1, 2, ..., 10$) 1 2 3 4 5 6 7 8 9 10	source impedances of node 1	Fault point locator	Error (%)
○●○●○○○○○○	1 p.u.	50.00	0
○●○●○○○○○○	2 p.u.	50.00	0
○●○●○○○○○○	3 p.u.	50.00	0
○●○●○○○○○○	5 p.u.	50.00	0
○●○●○○○○○○	10 p.u.	50.00	0

* 1 p.u. means the original source impedance of node 1, as shown in Table IX

* All 0 error means that the error is less than 0.01%.

Commonly, when applying the method to practical case, the realistic parameters involved may not be of high accuracy. So we give the sensitivity of the proposed method to system parameters in Table IV and Table V. In Table IV, a phase-A to ground fault occurs on the main line section 2-4 with resistance 100 Ω , and the fault point is 75% away from node 2. In Table V, a phase-A to ground fault occurs on the tapped line section 4-5 with resistance 100 Ω , and the fault point is 75% away from node 4. From Table IV and Table V, we can see that the proposed method is affected in some way, but it still shows pretty good results.

TABLE IV
COMPUTATIONAL RESULTS UNDER DIFFERENT PARAMETERS ERROR WHEN FAULT ON THE MAIN LINE SECTION 2-4

Influence factors	Fault Point Locator	Error (%)
The parameters involved are totally accurate	75.00	0
Line parameters error on fault section 2-4 is 5%	77.49	2.49
Line parameters error on fault neighboring section 2-3 is 5%	75.24	0.24
Line parameters errors on fault section 2-4 and on fault neighboring section 2-3 are both 5%	80.91	5.91

TABLE V
COMPUTATIONAL RESULTS UNDER DIFFERENT PARAMETERS ERROR WHEN FAULT ON THE TAPPED LINE SECTION 4-5

Influence factors	Fault Point Locator	Error (%)
The parameters involved are totally accurate	74.98	0.02
Line parameters error on fault section 4-5 is 5%	74.00	1.00
Line parameters error on fault neighboring section 2-4 is 5%	82.96	7.96
Line parameters errors on fault section 4-5 and on fault neighboring section 2-4 are both 5%	81.65	6.65

B. Simulation system 2

TABLE VI
TAPS LENGTH OF THE TWO SIMULATION SYSTEMS

Tap Section	System 1 (km)	System 2 (km)
2-3	100	20
4-5	50	10
6-7	150	30
8-9	100	20

TABLE VII
SIMULATION RESULTS UNDER DIFFERENT FAULT CONDITIONS

Fault No.	Fault location index ΔI_i ($i = 1, 2, ..., 10$) 1 2 3 4 5 6 7 8 9 10	Fault section selector	Fault point locator	Err (%)	Results from the original manuscript: Fault point locator	Results from the original manuscript: Error (%)
1	● ● ○ ○ ○ ○ ○ ○ ○ ○	1-2	5.00	0	5.00	0
2	● ● ○ ○ ○ ○ ○ ○ ○ ○	1-2	50.00	0	50.00	0
3	● ● ○ ○ ○ ○ ○ ○ ○ ○	1-2	95.00	0	95.00	0
4	● ● ○ ● ○ ○ ○ ○ ○ ○	2-3	**5.01**	**0.01**	**5.00**	**0**
5	● ● ○ ● ○ ○ ○ ○ ○ ○	2-3	50.01	0.01	49.99	0.01
6	● ● ○ ● ○ ○ ○ ○ ○ ○	2-3	**95.01**	**0.01**	**95.00**	**0**
7	○ ● ○ ● ○ ○ ○ ○ ○ ○	2-4	5.00	0	5.00	0
8	○ ● ○ ● ○ ○ ○ ○ ○ ○	2-4	50.00	0	50.00	0
9	○ ● ○ ● ○ ○ ○ ○ ○ ○	2-4	95.00	0	94.99	0.01
10	○ ● ○ ● ○ ● ○ ○ ○ ○	4-5	**4.98**	**0.02**	**4.99**	**0.01**
11	○ ● ○ ● ○ ● ○ ○ ○ ○	4-5	50.00	0	50.00	0
12	○ ● ○ ● ○ ● ○ ○ ○ ○	4-5	95.00	0	95.00	0
13	○ ○ ○ ● ○ ● ○ ○ ○ ○	4-6	5.00	0	5.00	0
14	○ ○ ○ ● ○ ● ○ ○ ○ ○	4-6	50.00	0	50.00	0
15	○ ○ ○ ● ○ ● ○ ○ ○ ○	4-6	95.00	0	95.00	0
16	○ ○ ○ ● ○ ● ○ ● ○ ○	6-7	**4.98**	**0.02**	**5.00**	**0**
17	○ ○ ○ ● ○ ● ○ ● ○ ○	6-7	**49.98**	**0.02**	**50.00**	**0**
18	○ ○ ○ ● ○ ● ○ ● ○ ○	6-7	95.00	0	95.00	0
19	○ ○ ○ ○ ○ ● ○ ● ○ ○	6-8	5.00	0	5.00	0
20	○ ○ ○ ○ ○ ● ○ ● ○ ○	6-8	50.00	0	50.00	0
21	○ ○ ○ ○ ○ ● ○ ● ○ ○	6-8	95.00	0	95.00	0
22	○ ○ ○ ○ ○ ● ○ ● ○ ●	8-9	**4.99**	**0.01**	**5.00**	**0**
23	○ ○ ○ ○ ○ ● ○ ● ○ ●	8-9	**49.97**	**0.03**	**49.99**	**0.01**
24	○ ○ ○ ○ ○ ● ○ ● ○ ●	8-9	**94.97**	**0.03**	**94.98**	**0.02**
25	○ ○ ○ ○ ○ ○ ○ ● ○ ●	8-10	4.99	0.01	4.99	0.01
26	○ ○ ○ ○ ○ ○ ○ ● ○ ●	8-10	50.00	0	50.00	0
27	○ ○ ○ ○ ○ ○ ○ ● ○ ●	8-10	95.00	0	95.00	0

*○ represents zero element.

*● represents non-zero element.

* All 0 error means that the error is less than 0.01%.

In realistic systems, many taps are necessarily short. To validate the proposed technique, a similar system with short taps is simulated. The simulation system 2 is exactly the same with simulation system 1, except for the taps length. The difference between their taps length is shown in Table VI.

The faults simulated are exactly the same as listed in Table I. The results are shown in Table VII. From the Table VII, the proposed technique shows very promising results for transmission lines with short taps, though the errors are a little higher than errors from transmission lines with long taps.

VI. CONCLUSIONS

This paper presents an accurate and efficient fault location technique for multi-terminal transmission lines. The nodal current unbalance $\Delta \boldsymbol{I}_{n\times 1}$, fault location index, is firstly defined, then, the special features of $\Delta \boldsymbol{I}_{n\times 1}$ for two different fault cases are derived by detailed theory analysis. The main conclusions of this paper are summarized as follows:

- When a fault occurs on the main line section $i-j$, $\Delta \boldsymbol{I}_{n\times 1}$ has two non-zero elements.
- When a fault occurs on the tapped line section $i-j$, $\Delta \boldsymbol{I}_{n\times 1}$ has three non-zero elements.
- Once the faulted section is identified, the exact fault point x can be obtained directly by (42), the computational burden of proposed approach is very low.
- The case studies verify that the proposed approach is robust and enough accurate for all tested faults.

The distinctive features of the proposed fault location technique are concluded as follows:

- It is an improvement that the proposed fault location technique for multi-terminal lines avoids the use of source impedances in the formulation.
- The proposed technique performs with very high accuracy for all types of faults at different fault locations. Classification of fault types and selection of fault phase are not required.
- The proposed technique is practically immune to the fault resistance and is free of pre-fault conditions.

REFERENCES

[1] Yuan Liao, "Fault location utilizing unsynchronized voltage measurements during fault", Electric Power Components & Systems, vol. 34, no. 12, December 2006, pp. 1283 – 1293.

[2] K. Takagi, Y. Yomakoshi, M. Yamaura, R. Kondow, and T. Matsushima, "Development of a new type fault locator using the one-terminal voltage and current data," *IEEE Trans. Power App. Syst*., vol. PAS-101, no. 8, pp. 2892–2898, Aug. 1982.

[3] L. Eriksson, M. M. Saha, and G. D. Rockefeller, "An accurate fault locator with compensation for apparent reactance in the fault resistance resulting from remote-end indeed" *IEEE Trans. Power App. Syst*., vol. PAS-104, no. 2, pp. 424–436, Feb. 1985.

[4] DONG XinZhou, SHI ShenXing, "Optimizing solution of fault location using single terminal quantities," *Sci China Ser E-Tech Sci*, vol. 51, no.6, pp-761-772, Jun.2008

[5] J. Izykowski, E. Rosolowski, and M. M. Saha, "Locating faults in parallel transmission lines under availability of complete measurements at one end," *Proc. Inst. Elect. Eng., Gen., Transmd Distrib.*, vol. 151, no. 2, pp. 268–273, Mar. 2, 2004.

[6] D. Novosel, D. G. Hart, E. Udren, and J. Garitty, “Unsynchronized two-terminal fault location estimation,” IEEE Trans. Power Del., vol. 11, no. 1, pp. 130–138, Jan. 1996.

[7] A. Gopalakrishnan, M. Kezunovic, S. M. McKenna, and D. M. Hamai, “ Fault location using distributed parameter transmission line model,” *IEEE Trans. Power Del*., vol. 15, no. 4, pp. 1169–1174, Oct. 2000.

[8] J.-A. Jiang, J.-Z. Yang, Y.-H. Lin, C.-W. Liu, and J.-C. Ma, “An adaptive PMU based fault detection/location technique for transmission lines-part I: Theory and algorithms,” IEEE Trans. Power Deliver, vol. 15, no. 2, pp.486–493, Apr. 2000.

[9] Eduardo G. Silveira and Clever Pereira, “Transmission Line Fault Location Using Two-Terminal Data Without Time Synchronization,” IEEE Trans. Power Del., vol. 22, no.1, pp.498-499, Feb, 2007.

[10] Y. Lin, C. Liu, and C. Yu, “A new fault locator for three-terminal transmission lines using two-terminal synchronized voltage and current phasors,” *IEEE Trans. Power Del*., vol. 17, no. 2, pp. 452–459, Apr. 2002.

[11] C. Yu, C. Liu, and Y. Lin, “A fault location algorithm for transmission lines with tapped leg—PMU based approach,” in *Proc. IEEE Power Eng. Soc. Summer Meeting*, Vancouver, BC, Canada, 2001, pp. 915–920.

[12] R. K. Aggarwal, D. V. Coury, A. T. Johns, and A. Kalam, “A practical approach to accurate fault location on extra high voltage teed feeders,” *IEEE Trans. Power Del*., vol. 8, no. 3, pp. 874–883, Jul. 1993.

[13] Cansın Y. Evrenosoglu, Ali Abur. Travelling Wave Based Fault Location for Teed Circuits. *IEEE Trans. Power Del*., VOL. 20, NO. 2, APRIL 2005.

[14] M. Abe, N. Otsuzuki, T. Emura, and M. Takeuchi, “Development of a new fault location system for multi-terminal single transmission lines,” *IEEE Trans. Power Del*., vol. 10, no. 1, pp. 159–168, Jan. 1995.

[15] T. Funabashi, H. Otoguro, Y. Mizuma, L. Dube, and A. Ametani,“Digital fault location algorithm for parallel double-circuit multi-terminal transmission lines,” *IEEE Trans. Power Del*., vol. 15, no. 2, pp. 531–537, Apr. 2000.

[16] J. V. H. Sanderson, R. G. R. Santana, and B. Al-Fakri, “Improved directional comparison based algorithm for protection of multi-terminal transmission lines,” *in Proc. 5th Int. Conf. Developments Power Syst. Protection*, 1993, vol. 368, pp. 153–156.

[17] S. M. Brahma, “Fault location scheme for a multi-terminal transmission line using synchronized voltage measurements,” *IEEE Trans. Power Del*., vol. 20, no. 2, pp. 1325–1331, Apr. 2005.

[18] Chih-Wen Liu, Kai-Ping Lien, Ching-Shan Chen, and Joe-Air Jiang, “A Universal Fault Location Technique for N-Terminal(N≥ 3)Transmission Lines” *IEEE Trans. Power Del*, vol. 23, no. 3, pp. 1366–1373, July. 2008.

[19] FAN Chunju DU Xiuhua LI Shengfang, et al. An Adaptive Fault Location Technique Based on PMU for Transmission Line. *IEEE PES General Meeting*, Tampa, FL, Jun. 2007

[20] Sukumar M. Brahma. New Fault-Location Method for a Single Multiterminal Transmission Line Using Synchronized Phasor Measurements. *IEEE Trans. Power Del.*, VOL. 21, NO. 3, JULY 2006

[21] Dennis Woodford. Introduction to PSCAD/EMTDC V4[R]. Manitoba, Canada. HVDC Research Center Inc. 2003.

APPENDIX I

The parameters of the six-terminal transmission lines are given in the following tables.

TABLE VIII
PARAMETERS OF THE LINES USED FOR SIMULATION

Section	Length (km)	R_1, X_1, B_1 (Ω/km)	R_0, X_0, B_0 (Ω/km)
1-2	100	R_1 =3.5744e-2	R_0 =3.6315e-1
2-4	120		
4-6	100		
6-8	80		
8-10	100		
2-3	100	X_1 =5.2676e-1 B_1 =3.2711e-6	X_0 =1.3264 B_0 =2.3226e-6
4-5	50		
6-7	150		
8-9	100		

TABLE IX
SOURCE IMPEDANCE OF THE SIMULATED SYSTEM

Power Source	Z_1 (Ω)	Z_0 (Ω)
$E_1 = 1\angle 0^0$	0.238+j5.72	2.738+j10
$E_5 = 1\angle 10^0$	0.155+j5.95	1.786+j7.58
$E_7 = 1\angle 20^0$	0.367+j6.84	3.256+j10.58
$E_9 = 1\angle 30^0$	0.132+j6.95	1.286+j8.58
$E_{10} = 1\angle 35^\circ$	0.338+j8.19	2.833+j11.12

BIOGRAPHIES

Quanyuan Jiang (M’10) received the B.S., M.S., and Ph.D. degrees in electrical engineering from Huazhong University of Science and Technology, Wuhan, China, in 1997, 2000, and 2003 respectively.

Since July 2003, he has worked at Zhejiang University, Hangzhou, China, as a Faculty, where he is currently a full Professor in the College of Electrical Engineering. His research interests include power system stability and control, optimization, and parallel computing in power systems, and integration of renewable energy resource into power system.

Bo Wang was born in Zhejiang, China in 1985. He received his B.S and M.S. degrees in the College of Electrical Engineering from Zhejiang University, Hangzhou, China in 2007 and 2010 respectively. Currently, Bo Wang is with Ningbo Electric Company of State Grid, China. His research interests are fault location in transmission network and the application of WAMS.

Xingpeng Li was born in Shandong, China in 1989. He received his B.S degree in the College of Electrical Engineering from Shandong University, Jinan, China in 2010. Currently, he is pursuing the master degree in the College of Electrical Engineering at Zhejiang University. His research interests are fault location, microgrid power energy management, integration of renewable energy resource into power system, and power system operation, control, and optimization.